

# A Continuum Approach to the Distribution of Plasma in a Pulsar Magnetosphere

Julian Faust

Department of Physics, Engineering Physics and Astronomy

Queen's University at Kingston

*Under the supervision of:* Dr. R. N. Henriksen

*Undergraduate Research Thesis*

2010 April



# Contents

---

List of Figures	v
<b>1 Introduction</b>	<b>1</b>
<b>2 PSR J0737-3039</b>	<b>3</b>
2.1 Basic Parameters . . . . .	3
2.2 Eclipse Light Curve . . . . .	3
<b>3 The Magnetosphere at Equilibrium</b>	<b>5</b>
<b>4 Magnetic Fields</b>	<b>9</b>
4.1 Oblique Rotating Dipole . . . . .	9
4.2 Deutsch Fields . . . . .	9
4.3 Plasma Fields . . . . .	10
<b>5 Numerical Density Calculation</b>	<b>11</b>
5.1 Input Parameters . . . . .	11
5.2 Output . . . . .	12
<b>6 Results and Discussion</b>	<b>13</b>
6.1 Dependence on . . . . .	13
6.2 Magnetic Dipole vs. Deutsch fields . . . . .	13
6.3 Comparison with McDonald and Shearer (2009) . . . . .	14
6.4 Comparison with Lyutikov and Thompson (2005) . . . . .	15
<b>7 Conclusions</b>	<b>23</b>
References	25

## CONTENTS

---



## LIST OF FIGURES

---

6.4 Using Lyutikov and Thompson's best  $t$  value = 75

# Introduction

## 1. INTRODUCTION

---

section 4, various possibilities in modelling the magnetic field are considered. Section 5 describes the computational methods used to generate data sets and plots. Finally, in section 6.4 we discuss our density distributions in the context of the eclipse light curve and the reasonably successful model due to Lyutikov and Thompson (2005).



# PSR J0737-3039

---

PSR J0737-0309 is the first known double pulsar binary system, and aside from being a laboratory for precise tests of General Relativity it has provided a unique opportunity to study the absorption of radio frequency radiation from one pulsar in the magnetosphere of the other.

## 2.1 Basic Parameters

Pulsar B's radius is taken to be  $\approx 10$  km, and its mass is about 1.25 solar masses. It orbits with A around their center of mass with a semimajor axis of  $8.8 \cdot 10^8$  m a eccentricity 0.088, with a period of 2.45 hours. A and B's spin periods are 23 ms and 2.8 s respectively, and both are visible in the radio spectrum<sup>1</sup>. B's dipole moment is estimated as approximately  $3.5 \cdot 10^{26}$  J/T.

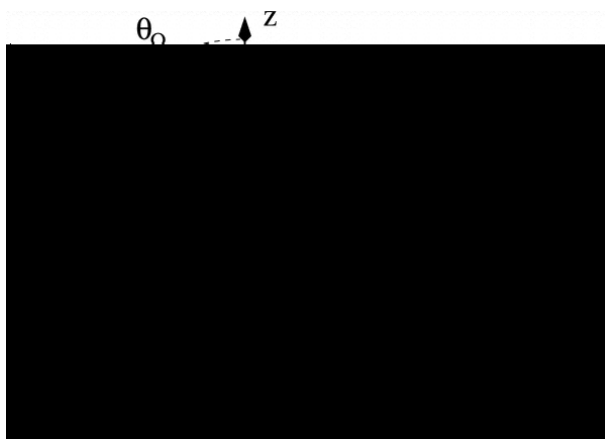


**Figure 2.1:** Geometry of the eclipse, with origin at pulsar B and z-axis normal to the orbital plane. The spin axis  $B$  makes an angle  $\theta_0$  with the z-axis, and the magnetic dipole moment  $B$  makes at an angle  $\theta$  to  $B$ . (Figure from Lyutikov and Thompson (2005))

## 2.2 Eclipse Light Curve

The orbit is nearly (but not quite) edge on as viewed from Earth, so that once per orbit pulses from A pass through B's magnetosphere with some impact parameter  $z_0$ . The intensity of radiation received from A is modulated in time over the  $\approx 30$ s eclipse, showing largely opaque periods as well as nearly transparent windows at the first and second harmonics of pulsar B's spin frequency (see e.g. 2.2). These features are explained fairly well by Lyutikov and Thompson (2005) using a simple geometric model of pulsar B's magnetosphere as a rigidly rotating oblique

---

<sup>1</sup>Breton et al. (2008)

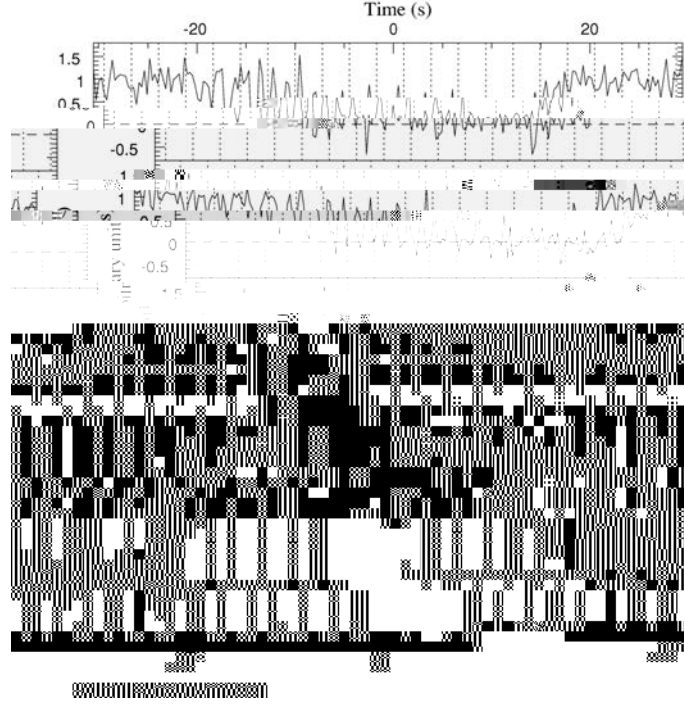


**Figure 2.2:** Light intensity curves from three eclipses of J0737-0309 A by B are shown; the bottom panel is the average of the three. The dotted vertical lines represent the timing of pulses from B. (McLaughlin et al., 2004)

magnetic dipole, with constant plasma density along those field lines with maximum extension between some inner and outer radius  $R < R_{max} < R_+$ , measured at the magnetic equator. Field lines closing inside or outside this radius are given zero density. These assumptions are contrary to those of this thesis, as our method gives varying density along field lines. Their model is successful enough, however, that a detailed study was carried out using our method with their best fit parameters wherever possible. The implications of our method in the context of Lyutikov and Thompson (2005) are discussed in section 6.4. They provide best fit values for the parameters  $R$ ,  $R_+$ , the angles  $\alpha$ ,  $\beta$  and  $\gamma$ , and the impact parameter  $z_0$  (see Fig. 2.1). Of primary interest to this thesis are  $R_+$  and  $\alpha$ , since the computation described in section 5 calculates a density profile but does not go as far as to simulate the eclipse.  $R_+$  can be used to limit the computation to a region comparable to the size of the magnetosphere (i.e. the half-width of the eclipsing material, which is determined from the duration of the eclipse and the orbital radius and period to be  $1.5 \cdot 10^7$  m). One needs such a limit, as the assumption of corotation breaks down at the light cylinder. Additionally, under the strict assumption of corotation the density calculation diverges for field lines approaching the light cylinder, and the maximum density attained in a calculation depends strongly on the limit  $R_+$ . Lyutikov and Thompson's best fit value for the angle  $\alpha$  between the dipole moment and the rotation axis is  $75^\circ$ , and this is taken as a starting point for our investigations.

# The Magnetosphere at Equilibrium

---

The computational tool making this study of the magnetosphere possible is an integral of the motion due to Henriksen and Rayburn (1973); some key points of the derivation are summarized here. The notation primarily follows that of Fock (1964), taking the (+ { { }) convention for the Minkowski metric.

We consider the region surrounding a pulsar isolated from external gravitational influences (in the context of PSR J0737-3039, we neglect the effect of pulsar A's gravity on B's magnetosphere). The surrounding matter is treated as a single fluid plasma with stress-energy-momentum tensor (see Fock (1964))

$$T_M = (\rho + p/c^2)u^\mu u_\mu - pg : \quad (3.1)$$

where  $p$  is the pressure,  $\rho$  is the total mass density in the local inertial frame (including the mass equivalent of the plasma's compressional potential energy), and  $u^\mu$  is the four velocity.

The metric  $g_{\mu\nu}$  is taken to be the Schwarzschild metric, with line element

$$ds^2 = g_{\mu\nu} dx^\mu dx^\nu = \left(1 - \frac{2GM}{rc^2}\right) c^2 dt^2 - \frac{1}{1 - \frac{2GM}{rc^2}} dr^2 - r^2(d\theta^2 + \sin^2\theta d\phi^2): \quad (3.2)$$

Defining

$$\alpha = \frac{1}{1 - \frac{2GM}{rc^2}}; \quad (3.3)$$

the four velocity is

$$\begin{aligned} u^\mu &= \rho = \frac{dx^\mu}{dt} \\ &= \alpha \frac{1}{1 - \frac{r^2 \dot{\theta}^2 + r^2 \sin^2\theta \dot{\phi}^2}{c^2}}: \end{aligned} \quad (3.4)$$

Under the assumption that the plasma corotates with the pulsar, this simplifies to

$$u^\mu = \alpha \frac{1}{1 - \frac{r^2 \sin^2\theta \dot{\phi}^2}{c^2}}: \quad (3.5)$$

This implies a light cylinder radius of  $R_{lc} = \frac{c}{\dot{\phi}}$ , which is close to the value  $\frac{c}{\dot{\phi}}$  seen throughout the literature since  $\dot{\phi} \approx (1 - 3 \times 10^{-5}) \text{ rad/s}$  at this radius.

### 3. THE MAGNETOSPHERE AT EQUILIBRIUM

---

The use of the Schwarzschild metric in describing the geometry around a pulsar is justified under several assumptions:

It is a vacuum solution, so is a good approximation only if the total gravitational effect of the magnetosphere is negligible compared to that of the pulsar. We believe this to be the case, since the plasma is many orders of magnitude less dense than a neutron star interior.

It assumes a spherically symmetric mass distribution as the source of gravitation. In reality the mass distribution is distorted due to centrifugal effects.

It neglects the effects of the pulsar's rotation on the geometry, so we require that the pulsar's angular momentum  $J$  is not too large. A more complex treatment could be done using the Kerr metric, which reduces to the Schwarzschild metric in the limit that  $\frac{J}{Mc^2r} \ll 1$ . The angular momentum of a pulsar is difficult to predict since the equation of state is unknown, and thus the moment of inertia cannot be calculated. As a rough estimate, we idealize pulsar B as a uniform sphere (radius  $\approx 10$  km) with moment of inertia  $I = \frac{2}{5}M_B R_B^2$  to find

$$\frac{J}{Mc^2r} \approx \frac{2}{5} \frac{R_B^2}{c} \frac{B}{r} \approx 3 \times 10^{-5} \frac{R_B}{r} \quad (3.6)$$

which in our calculation, is at most  $3 \times 10^{-6}$ . In light of this, the gravitational effects of pulsar B's rotation should be negligible; however, it should be noted that the moment of inertia is unknown by a large factor, and the Kerr geometry will begin to become significant for faster-spinning pulsars.<sup>1</sup>

Under these assumptions, we proceed in using the Schwarzschild metric in the corotating frame with the understanding that the calculation is restricted to the region  $R_{pulsar} < r < R_{lc}$ .  $R_{lc}$  is the "light cylinder" beyond which the assumption of corotation would imply velocities greater than  $c$ . Due to the strong magnetic field, we suppose that charged particles are confined to magnetic field lines, executing helical motion. Field lines that close a reasonable distance within the light cylinder may then be capable of supporting an equilibrium density of plasma.

Adding the electromagnetic field tensor to the equation 3.1 gives the total mass-energy-momentum tensor  $T$ . The equations of motion follow from the conservation laws given by setting the covariant derivative of  $T$  equal to zero.

$$\begin{aligned} T &= T_M + T_E \\ T_{; \alpha} &= 0 \end{aligned} \quad (3.7)$$

---

<sup>1</sup>The double pulsar system may allow a unique opportunity to measure the moment of inertia of pulsar A



### 3. THE MAGNETOSPHERE AT EQUILIBRIUM

---



## 4. MAGNETIC FIELDS

(4.1)

Here the polar angle  $\theta$  refers to the axis of rotation,  $\alpha$  is the angle between the rotation axis and the effective magnetic dipole moment, and  $\tau = \frac{r}{R_{lc}} t$  (See Higgins (1996)).

The magnetic Deutsch field reduces to a magnetic dipole for  $R_{pulsar} \ll r \ll R_{lc}$ . Considering that the eclipsing material of pulsar B has a half-width of  $1.4 \cdot 10^7 \text{ m}^1$  and the light cylinder is about  $1.3 \cdot 10^8 \text{ m}$ , the Deutsch field will begin to give distinct results in the outer magnetosphere.

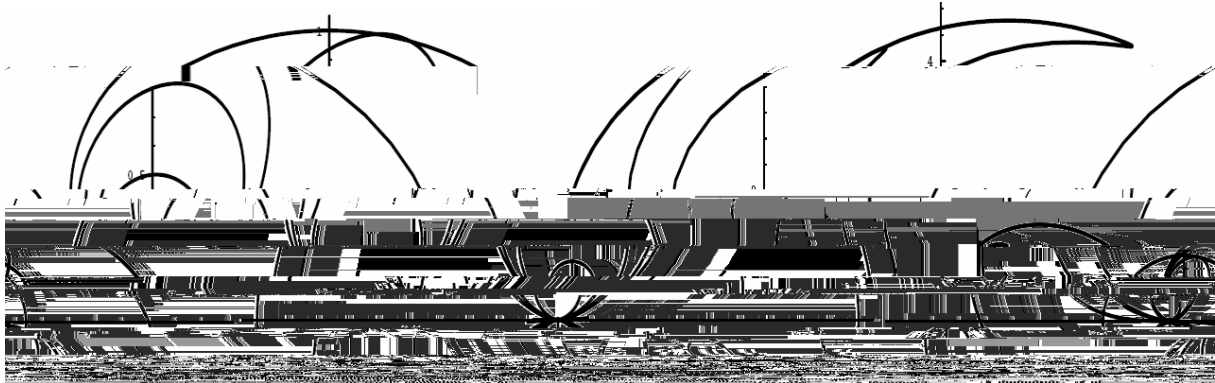


**Figure 4.1:** A selection of Deutsch magnetic field lines that close within the light cylinder is shown at left, where the large circle represents the light cylinder. At right, a selection of open Deutsch magnetic field lines is shown on a larger scale, where the small circle now represents the light cylinder. ( Figures from Henriksen and Higgins (1997))

Deutsch fields have been used in describing the exterior of a pulsar, for example by Henriksen and Higgins (1997), Quadir et al. (1980) and McDonald and Shearer (2009).

### 4.3 Plasma Fields

The Deutsch fields are vacuum solutions to Maxwell's Equations, and thus completely neglect the electromagnetic fields due to the flow of plasma in the magnetosphere. The plasma fields could in principle be added to the Deutsch fields by the principle of superposition; the problem is then to self-consistently solve for the charge and current densities and electromagnetic fields. This is a daunting task both analytically and computationally, and is beyond the scope of this paper. See McDonald and Shearer (2009) for a 3D computation that self-consistently finds equilibrium charge distributions using a superposition of Deutsch fields and plasma fields.

<sup>1</sup>Lyutikov and Thompson (2005)



# Numerical Density Calculation

---

A major analytical difficulty is the loss of symmetry when the angle between the dipole moment and the axis of rotation is nonzero, which seems to be necessary in describing a real pulsar. For

## 5. NUMERICAL DENSITY CALCULATION

---

The reference points should be chosen with the limiting radius in mind, since the field lines

# Results and Discussion

---

## 6.1 Dependence on

Without knowledge of the equation of state of the plasma, we must choose a value of  $\gamma$  in the relation  $p \propto \rho^\gamma$ . Three choices of  $\gamma$  between 1 and 2, and the corresponding density distributions are shown in Figure 6.1.

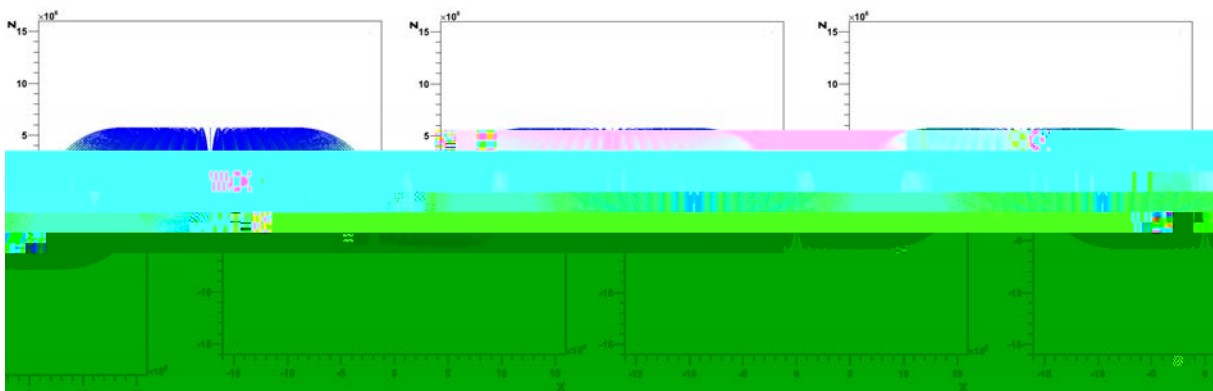


Figure 6.1: The axisymmetric case is shown for three values of  $\gamma$  :  $\gamma = 1$ :

## 6. RESULTS AND DISCUSSION

---



**Figure 6.2:** The axisymmetric case, with the magnetic dipole calculation at left and the calculation using Deutsch fields at right, for field lines that close within  $1.5 \cdot 10^7$ m.

Figure 6.3 shows the dipole field (left) and the Deutsch field in the extreme case in which the dipole moment is orthogonal to the rotation axis ( $\theta = \pi/2$ ). Field lines closing within  $0.5R_{IC}$  are plotted. The distortion in the dipolar structure of the Deutsch fields can clearly be seen for fieldlines extending along the z-axis, while the field lines near the rotational equator  $z = 0$  do not extend as far radially and more or less maintain their dipolar shape. Note that the upper right panel of figure 6.3 shows the Deutsch magnetosphere to be narrower horizontally than the dipole fields; this is due to the Deutsch fields beginning to twist at large radii, as seen by comparing the bottom two panels. The viewing angle in the top right panel does not necessarily show the Deutsch magnetosphere at its maximum width, as is the case in the top left panel.

### 6.3 Comparison with McDonald and Shearer (2009)

McDonald and Shearer (2009) use a superposition of Deutsch fields and plasma fields in a 3D simulation to find stable charge distributions by self-consistently moving charges around until a stability condition is met. It is important to recognize the distinction between this type of simulation and the one carried out in this thesis: McDonald and Shearer (2009) find distributions of non-neutral plasma in which the electromagnetic forces are balanced, while our calculation finds mass distributions when the thermal, gravitational and centrifugal effects are balanced (under the assumption that the electrostatic effects of the charge separation are negligible). A full simulation including these effects in a plasma density calculation would be an ambitious, but potentially worthwhile endeavour.



**Figure 6.3:** The orthogonal case, restricting field lines to one half of the light cylinder radius,  $6.7 \cdot 10^7$ m. The left figures shows the dipole fields and the right figures shows the Deutsch fields; the bottom figures are the same calculations rotated by  $90^\circ$  so that the dipole moment is out of the page. Using  $\beta = 1.8$ , the dipole calculation had a relative maximum and minimum density of 250 and  $1 \cdot 10^{-4}$ , while the maximum and minimum for the Deutsch field calculation were 245 and  $1 \cdot 10^{-3}$  respectively.

## 6.4 Comparison with Lyutikov and Thompson (2005)

Lyutikov and Thompson model the density in the magnetosphere as being concentrated uniformly on a set of field lines with maximum extension within a fairly narrow range  $R < R_{max} < R_+$ . The assumption of constant density along field lines is contrary to our approach. Further, their criterion for the maximum radius is based on estimates of the "size" of the magne-

## 6. RESULTS AND DISCUSSION

---

tosphere, and so they measure this radius with respect to the magnetic equator; as a result the limiting fieldlines, and thus the density distribution, are axially symmetric about the magnetic axis. Equations 3.9 and 3.10 suggest that the density distribution should be axially symmetric about the rotation axis, at least for initial points satisfying this symmetry; however when we restrict the calculation to field lines that close within a certain radius we obtain a density distribution that is not symmetric about either axis. When our calculation is restricted to a similar maximum radius we find relative densities ranging from 1 at the initial radius  $r = 100\text{km}$  down a minimum of about  $1 \cdot 10^{-4}$  (blue) before increasing to about 4.5 (red), when the parameter  $\alpha = 1.8$ . Lower values of  $\alpha$  have the effect of increasing the maximum and decreasing the minimum. Given these considerations, we raise two issues with the model due to Lyutikov and Thompson (2005):

1. Their selection of which field lines to include uses a maximum distance measured along the magnetic equator, rather than along the equator of rotation. In our model we suppose that the ability of a field line to support an equilibrium plasma density depends on how closely it approaches to the light cylinder, and so the shape of the limiting field lines we include depends on the angle  $\theta$ . In fitting the angle  $\theta$ , Lyutikov and Thompson's magnetosphere stays the same shape.
2. Their model neglects to consider the equilibrium density along field lines, and assuming constant density seems to be a gross oversimplification.

As a possible explanation of their results, we note that the high density regions we calculate seem to lie approximately in a plane, which is not normal to the dipole moment or the axis of rotation, but is inclined somewhere between. If this was primarily the matter affecting the eclipse, then under Lyutikov and Thompson's assumptions the dipole moment is normal to this plane, which leads to an underestimation of the angle  $\theta$ . One can then ask if there is angle  $\theta$ , in our model, which gives a density distribution concentrated around a plane normal to Lyutikov and Thompson's best fit for the parameter  $\alpha$ , in the hopes that our density distribution can reproduce the eclipse light curve with a different value of  $\alpha$ . Figures 6.7 and 6.8 show calculations with the Deutsch fields for  $\alpha = 80$  and  $\alpha = 85$  respectively. As  $\alpha$  approaches 90 the distribution becomes complicated, but we attempt to draw a line (really a plane extending into the page) around which the density distribution is roughly centered.

This idea weakly suggests that the angle  $\theta$  is closer to 90 than predicted by Lyutikov and Thompson (2005), though a detailed study is clearly necessary since our density curves are drastically different than theirs.



## 6. RESULTS AND DISCUSSION

---

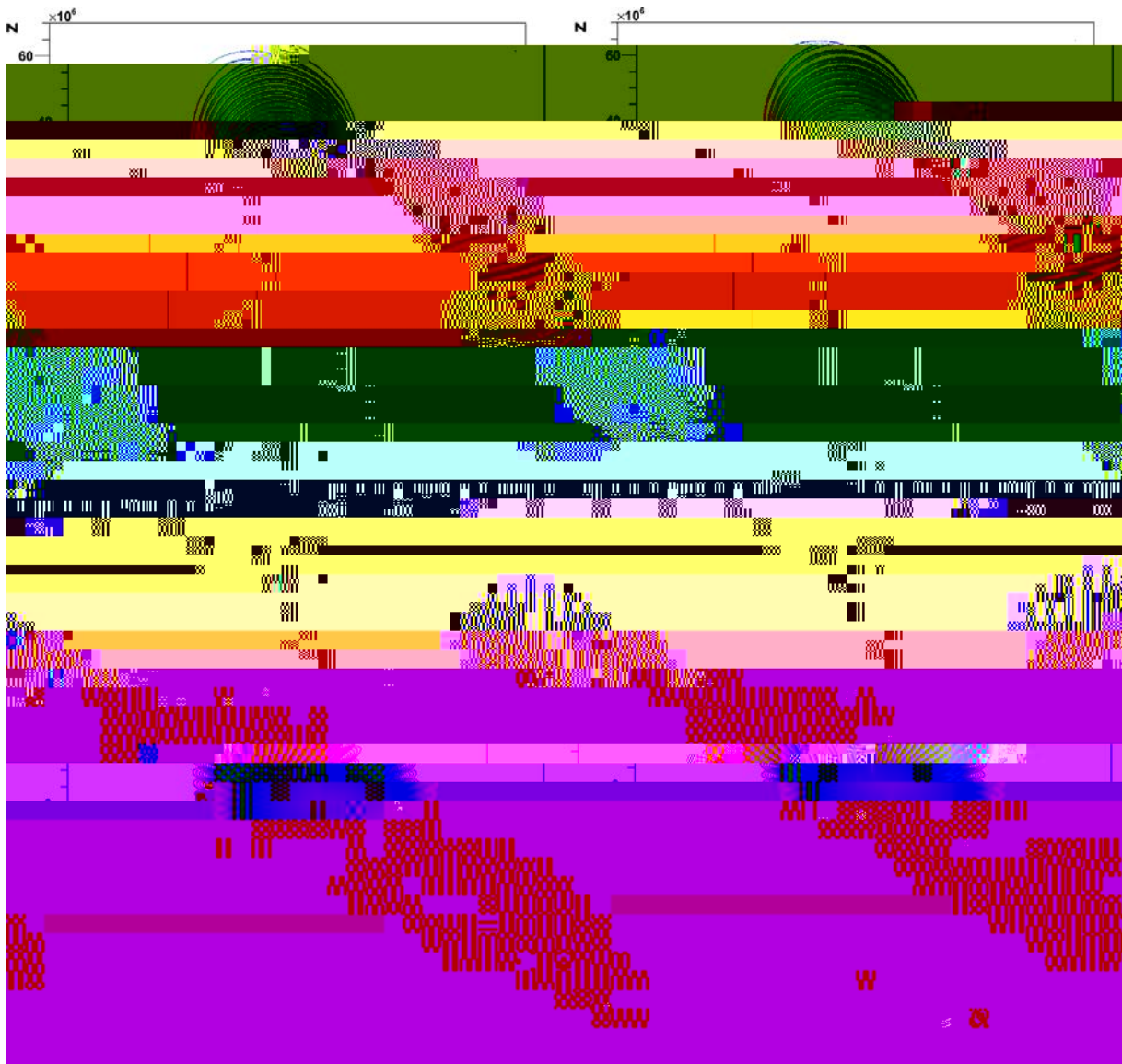


**Figure 6.5:** Using the same parameters as in 6.4, but restricting the field lines to those close within one quarter of the light cylinder radius, as measured at the rotational equator. Significant differences between the fields are still seen. The bottom frames show the same calculations rotated by  $90^\circ$ . In the dipole calculation the relative density reached a maximum of 36 and a minimum of  $3.5 \cdot 10^{-4}$ , and in the Deutsch field calculation it reached a maximum of 35.9 and a minimum of  $7.7 \cdot 10^{-4}$ .





**Figure 6.6:** Once again using the same parameters as in 6.4, we now restrict the field lines to those close within  $1.5 \cdot 10^7 \text{ m} \approx 0.11 R_{IC}$ , as measured at the rotational equator. The fields appear similar at this scale. The bottom frames show the same calculations rotated by  $90^\circ$ . In the dipole calculation the relative density reached a maximum of 4.61 and a minimum of  $9.5 \cdot 10^{-4}$ , and in the Deutsch field calculation it reached a maximum of 4.63 and a minimum of  $9.4 \cdot 10^{-4}$ .

## 6. RESULTS AND DISCUSSION

---

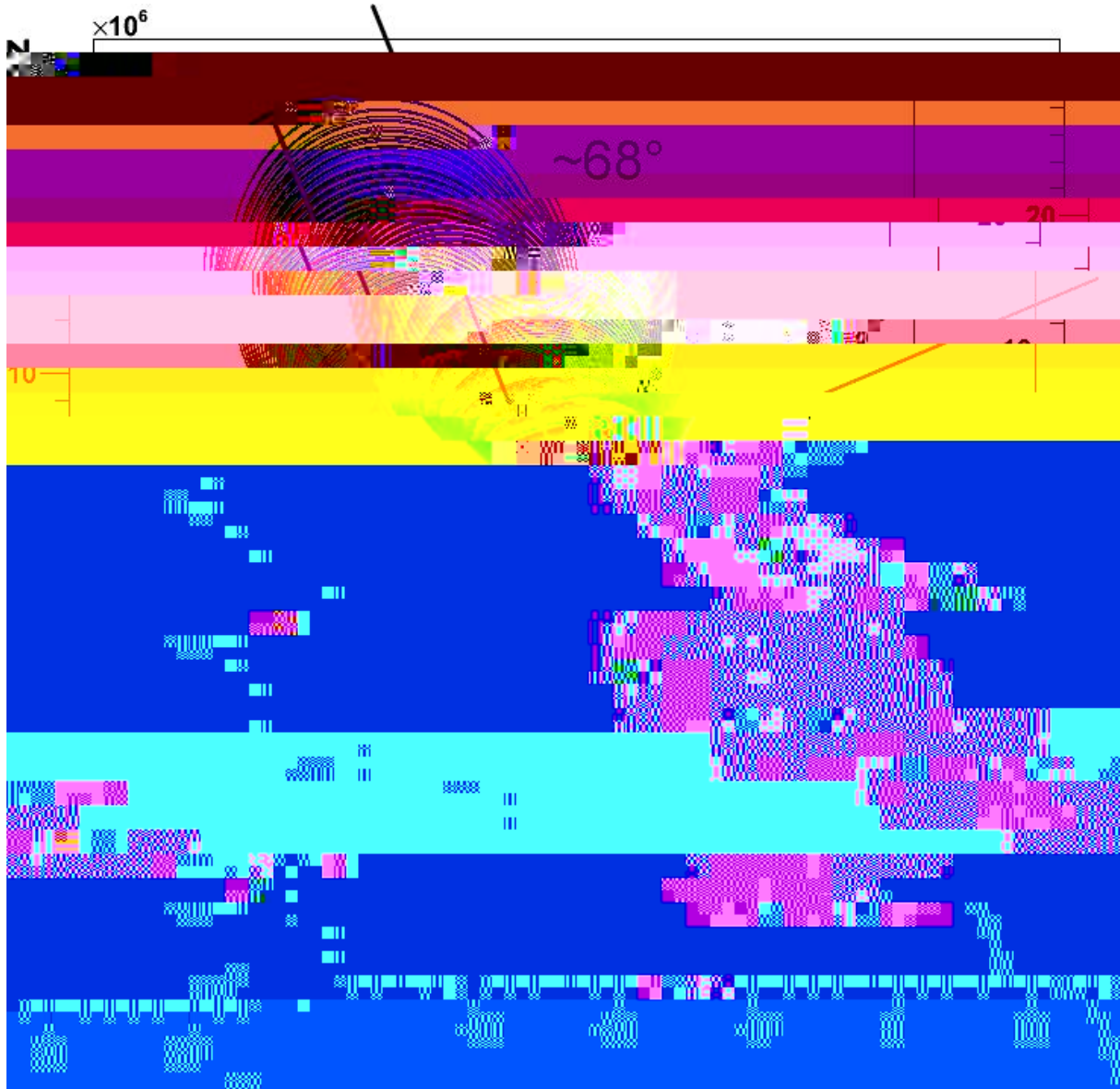


**Figure 6.7:** The Deutscherfeld lines closing within  $1.5 \cdot 10^7$  m are shown for  $\theta = 80^\circ$ . A line is drawn representing a plane about which the density is roughly centered. A perpendicular line represents the normal to this plane, which Lyutikov and Thompson's analysis implicitly takes to coincide with the dipole moment. We find this line to be at an angle of about  $68^\circ$ , though placement of the line is very subjective.

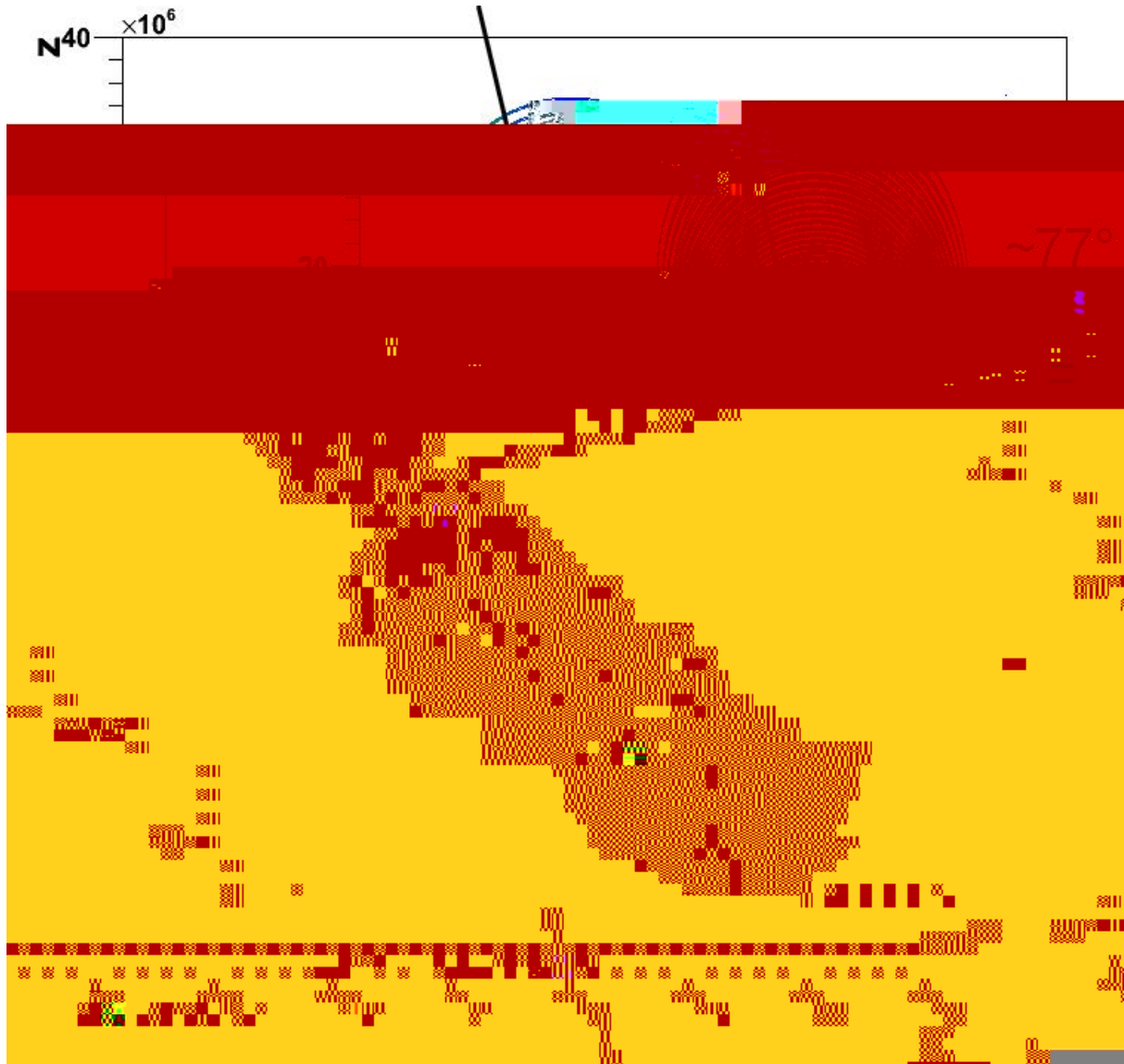


**Figure 6.8:** The Deutsch field lines closing within  $1.5 \cdot 10^7 \text{m}$  are shown for  $\beta = 85$ . A line is drawn representing a plane about which the density is roughly centered, but in this case the distribution is more complicated and the uncertainty in the slope is even larger. We give a value of about  $77^\circ$  for angle the normal to this plane makes with the rotation axis, though we recognize that the distribution takes on a new structure as  $\beta$  approaches  $90^\circ$ .

## 6. RESULTS AND DISCUSSION

---

## Conclusions

---

Our approach is novel to that in the literature, and gives results inconsistent with the ideas of Lyutikov and Thompson (2005) in particular. The shape of the absorbing material, as well as the plasma density distribution within it, is seen to change with the angle  $\theta$ . The density along field lines closing within some radius decreases away from the pulsar until the effects of corotation become significant and the density rises dramatically. It is clear that a full simulation of the eclipse light curve, along with an independent fitting of parameters, is necessary in order to fully evaluate our model in the context of the pulsar B. Our results differ drastically from Lyutikov and Thompson's, so it is not clear whether or not a best fit to our model would provide a slight modification of their parameters or a completely different set of parameters.

Within the radius  $r = 1.5 \times 10^7$

## 7. CONCLUSIONS

---

